Engineering Physics
2017; 1(2): 40-45
http://www.sciencepublishinggroup.com/j/ep
doi: 10.11648/j.ep.20170102.12

Structural Design to Maximum Radiating Power of Langevin Bolted Ultrasonic Transducer

Pak Myong-Il[1, *], Ri Ui-Hwan[1], An Yong-Nam[2]

[1]Electronic Material Institute of Kim Il Sung University, Taesong District, Pyongyang, Democratic People's Republic of Korea

[2]Cutting-Edge Technology Development Institute of Kim Il Sung University, Taesong District, Pyongyang, Democratic People's Republic of Korea

Email address:

ryongnam15@yahoo.com (P. Myong-Il), ryongnam16@yahoo.com (Ri Ui-Hwan), ryongnam17@yahoo.com (An Yong-Nam)

[*]Corresponding author

To cite this article:

Pak Myong-Il, Ri Ui-Hwan, An Yong-Nam. Structural Design to Maximum Radiating Power of Langevin Bolted Ultrasonic Transducer. *Engineering Physics.* Vol. 1, No. 2, 2017, pp. 40-45. doi: 10.11648/j.ep.20170102.12

Received: November 28, 2016; **Accepted**: March 30, 2017; **Published**: May 5, 2017

Abstract: Langevin bolted transducers (BLT) with two piezoelectric ceramics inserted between the front and rear plates are widely used in ultrasonic cleaner transducers and components of underwater acoustic antennas for a fish finder [1, 2]. And it is very important to attain a maximum ratio of vibrating velocities of the front and rear plates of transducers in radiating medium by choosing the optimal dimension of the front and rear plates of ultrasonic transducers. Prior studies introduced the vibrating mode analysis of BLT using FEM analysis and ultrasonic applications [3, 4, 5]. But study about the detailed structural design of transducers with the maximum vibrating velocity ratio of the front and back plates in the radiating medium based on the electromechanical equivalent circuit analysis is hardly found. In this paper we identified the optimal geometrical dimension of the front and rear plates of transducers with maximum vibrating velocity ratio for 20kHz of working frequency and applied FEM analysis using the ANSYS software. These are based on the analysis of 1-D longitudinal vibrating equivalent circuit for BLT inserted two piezoceramics between the front and rear plates. The front plate is conical shaped and rear plate is cylindrical shaped and these are consisted of different materials.

Keywords: Langevin Bolted, Ultrasonic Transducer, Equivalent Circuit, ANSYS

1. Equivalent Circuit Analysis of BLT

The geometrical structure of BLT is shown in the Figure 1.

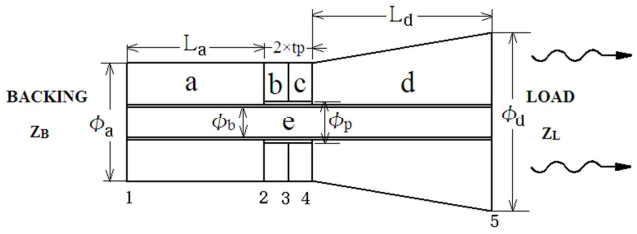

Figure 1. *Geometrical structure of BLT.*

As shown in the Figure 1, the rear plate a is made of steel and has a diameter of Φ_a=50mm and length of L_a, the front plate d is made of aluminum and has a diameter of Φ_d=80mm, Φ_a=50mm on front and back sides respectively and length of L_d disk-type piezoceramic elements b, c are made of PZT-M material with outer diameter of Φ_a=50mm, inner diameter of Φ_p=13mm and thickness of t_p=5mm, the bolt e is made of stainless steel and has a diameter of Φ_b=10mm. The front radiating medium is water and back radiating medium is air.

First, we conducted a MATLAB simulation to obtain geometrical dimensions of the front and rear plates with maximum ratio of vibrating velocity of the front and back sides based on the equivalent circuit analysis of longitudinal and one-dimensional vibration in radiating medium of boltless Langevin transducer. Second, we compared it with the analysis result of BLT (Langevin bolted ultrasonic transducer) using ANSYS software. The Electromechanical equivalent circuit [6, 7, 8, 9] of boltless Langevin transducer as one dimensional case can be easily analyzed but the equivalent circuit of BLT [10, 11, 12] is complicated due to the effect of bolt-joint, so we applied the ANSYS software to its analysis.

An electromechanical equivalent circuit consisted of four terminal network corresponding to the geometrical structure of boltless Langevin transducer is shown in the Figure 2.

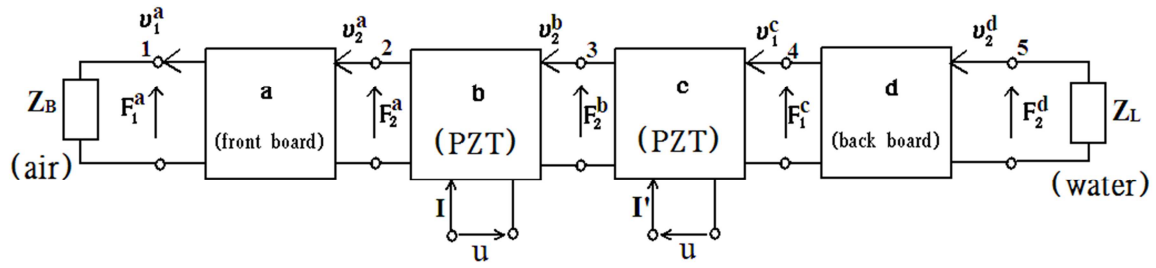

Figure 2. *Electromechanical equivalent circuit of Langevin transducer.*

In Figure 2, $F_1^a, F_2^a, F_2^b, F_1^c, F_2^d, \vartheta_1^a, \vartheta_2^a, \vartheta_2^b, \vartheta_1^c$ and ϑ_2^d are the active forces and vibrating velocities in the sides 1,2,3,4 and 5 of BLT in the Figure 1. And I and u are the electric current and voltage in the piezoceramics respectively.

The equivalent circuit parameters $z_{11}^a, z_{12}^a, z_{21}^a$ and z_{22}^a for the back plate, $z_{11}^b, z_{12}^b, z_{21}^b, z_{22}^b, z_{11}^c, z_{12}^c, z_{21}^c$ and z_{22}^c for PZT, $z_{11}^d, z_{12}^d, z_{21}^d$ and z_{22}^d for the front plate and Z_L, Z_B for characteristic impedance of the front and back radiating sides are shown in the equation (1).

$$Z_{11}^a = \mathrm{j}\cdot Z_a\cdot\cot(\mathrm{k}_a\cdot \mathrm{L}_a);\ Z_{12}^a = -\mathrm{j}\cdot Z_a\cdot\mathrm{cosec}(\mathrm{k}_a\cdot \mathrm{L}_a);$$

$$Z_{21}^a = -Z_{12}^a;\ Z_{22}^a = -Z_{11}^a;$$

$$Z_{11}^b = Z_{11}^c = \mathrm{j}(\frac{Z_0}{\sin(\mathrm{k}\cdot t_p)} - Z_0\cdot\tan\frac{(\mathrm{k}\cdot t_p)}{2} + \frac{1}{\omega \mathrm{c}1});$$

$$Z_{12}^b = Z_{12}^c = -\mathrm{j}(\frac{Z_0}{\sin(\mathrm{k}\cdot t_p)} + \frac{1}{\omega \mathrm{c}1});$$

$$\mathrm{Z}_{21}^b = Z_{21}^c = -Z_{12}^b = -Z_{12}^c;\ \mathrm{Z}_{22}^b = Z_{22}^c = -Z_{11}^b = -Z_{11}^c; \quad (1)$$

$$Z_{11}^d = \mathrm{j}\cdot Z_d\cdot[\cot(\mathrm{k}_d\cdot \mathrm{L}_d) - (1-\mathrm{N}_r)/(\mathrm{k}_d\cdot L_d)];$$

$$Z_{12}^d = -\mathrm{j}\cdot Z_d\cdot \mathrm{N}_r\cdot\mathrm{cosec}(\mathrm{k}_d\cdot \mathrm{L}_d);$$

$$Z_{21}^d = -\mathrm{Z}_{12}^d;\ Z_{22}^d = -jZ_d\mathrm{N}_r[(\mathrm{N}_r\cot(\mathrm{k}_d\cdot \mathrm{L}_d) + (1-\mathrm{N}_r)/(\mathrm{k}_d\cdot L_d)];$$

$$Z_L = \rho_L c_L s_d\{[1-2J_1(k_L\emptyset_d)/(k_L\emptyset_d)] + j2S_1(k_L\emptyset_d)/(K_L^2\cdot\emptyset_d^2)\};$$

$$Z_B = \rho_B c_B s_a\{[1-2J_1(k_L\emptyset_a)/(k_L\emptyset_a)] + j2S_1(k_L\emptyset_a)/(K_L^2\cdot\emptyset_a^2)\};$$

Here

$$k_a = \omega/c_a, Z_a = \rho_a c_a s_a, s_a = \pi(\emptyset_a^2 - \emptyset_\mathrm{b}^2)/4, c_a = \sqrt{E_a/\rho_a},$$

$$k_d = \omega/c_d,\ Z_d = \rho_d c_d s_d, s_d = \pi(\emptyset_d^2 - \emptyset_\mathrm{b}^2)/4, c_d = \sqrt{E_d/\rho_d}, \mathrm{N}_r = \emptyset_d/\emptyset_a;$$

$$\mathrm{k} = \omega/c,\ Z_0 = \rho\ \mathrm{c}\ \mathrm{s}, \mathrm{c}1 = -c_0/N^2, N = \frac{d_{33}\cdot s}{t_p\cdot s_{33}^E}, \mathrm{s} = \pi(\emptyset_a^2 - \emptyset_p^2)/4,$$

$$\mathrm{c} = 1/\sqrt{\rho\cdot s_{zz}^d}, S_{zz}^d = (\frac{1}{S_{33}^E} + \frac{d_{33}^2}{\varepsilon_{zz}^S\cdot S_{33}^E\cdot S_{33}^E})^{-1}, \mathrm{c}_0 = \mathrm{s}\cdot\varepsilon_{zz}^s/t_p,$$

$$\varepsilon_{zz}^s = \varepsilon_{33}^T - \mathrm{d}_{33}^2/\mathrm{s}_{33}^E, k_L = \omega/c_L, k_B = \omega/c_B,$$

(J_1: 1-D Bessel function, S_1: 1-D Strobe function).

The equivalent circuit equation corresponding to the electromechanical equivalent circuit of Langevin transducer shown in the Figure 2 which radiates in the medium is shown in the equation (2).

$$\begin{cases} \mathrm{F}_1^a = \mathrm{z}_{11}^a\cdot\vartheta_1^a + \mathrm{z}_{12}^a\cdot\vartheta_2^a = Z_\mathrm{B}\cdot\vartheta_1^a \\ \mathrm{F}_2^a = \mathrm{z}_{21}^a\cdot\vartheta_1^a + \mathrm{z}_{22}^a\cdot\vartheta_2^a \end{cases}$$

$$\begin{cases} \mathrm{F}_1^b = \mathrm{z}_{11}^b\cdot\vartheta_1^b + \mathrm{z}_{12}^b\cdot\vartheta_2^b + \mathrm{Nu} \\ \mathrm{F}_2^b = \mathrm{z}_{21}^b\cdot\vartheta_1^b + \mathrm{z}_{22}^b\cdot\vartheta_2^b + \mathrm{Nu} \\ \mathrm{I} = \mathrm{j}\omega \mathrm{c}_0\mathrm{u} - \mathrm{N}(\vartheta_2^b - \vartheta_1^b) \end{cases} \quad (2)$$

$$\begin{cases} \mathrm{F}_1^c = -\mathrm{z}_{11}^c\cdot\vartheta_1^c - \mathrm{z}_{12}^c\cdot\vartheta_2^c + \mathrm{Nu} \\ \mathrm{F}_2^c = -\mathrm{z}_{21}^c\cdot\vartheta_1^c - \mathrm{z}_{22}^c\cdot\vartheta_2^c + \mathrm{Nu} \\ \mathrm{I}' = \mathrm{j}\omega \mathrm{c}_0\mathrm{u} + \mathrm{N}(\vartheta_2^c - \vartheta_1^c) \end{cases}$$

$$\begin{cases} \mathrm{F}_1^d = \mathrm{z}_{11}^d\cdot\vartheta_1^d + \mathrm{z}_{12}^d\cdot\vartheta_2^d \\ \mathrm{F}_2^d = \mathrm{z}_{21}^d\cdot\vartheta_1^d + \mathrm{z}_{22}^d\cdot\vartheta_2^d = -Z_L\cdot\vartheta_2^d \end{cases}$$

The equation (2) leads to the equation (3): if expressed in the matrix form considering the vibration rate and the continuity of acting forces.

$$\begin{vmatrix} \mathrm{z}_{11}^a - z_B & \mathrm{z}_{12}^a & 0 & 0 & 0 \\ \mathrm{z}_{21}^a & \mathrm{z}_{22}^a - \mathrm{z}_{11}^b & -\mathrm{z}_{12}^b & 0 & 0 \\ 0 & \mathrm{z}_{21}^b & \mathrm{z}_{22}^b + \mathrm{z}_{22}^c & \mathrm{z}_{21}^c & 0 \\ 0 & 0 & -\mathrm{z}_{12}^c & -\mathrm{z}_{11}^c - \mathrm{z}_{11}^d & -\mathrm{z}_{12}^d \\ 0 & 0 & 0 & \mathrm{z}_{21}^d & \mathrm{z}_{22}^d + z_L \end{vmatrix} \times$$

$$\begin{vmatrix} \vartheta_1^{\mathrm{a}} \\ \vartheta_2^{\mathrm{a}} \\ \vartheta_2^{\mathrm{b}} \\ \vartheta_1^{\mathrm{c}} \\ \vartheta_2^{\mathrm{d}} \end{vmatrix} = \begin{vmatrix} 0 \\ \mathrm{Nu} \\ 0 \\ -\mathrm{Nu} \\ 0 \end{vmatrix} \tag{3}$$

From the equation (3), the transducer's frequency equation and the vibrating velocity amplitude of the front and back radiating sides can be written as the equation (4).

$$|D| = 0;\ v_1^a = |D_1|/|D|;\ v_2^d = |D_5|/|D| \tag{4}$$

Here

$$\mathrm{D} = \begin{vmatrix} \mathrm{z}_{11}^{\mathrm{a}} - z_B & \mathrm{z}_{12}^{\mathrm{a}} & 0 & 0 & 0 \\ \mathrm{z}_{21}^{\mathrm{a}} & \mathrm{z}_{22}^{\mathrm{a}} - \mathrm{z}_{11}^{\mathrm{b}} & -\mathrm{z}_{12}^{\mathrm{b}} & 0 & 0 \\ 0 & \mathrm{z}_{21}^{\mathrm{b}} & \mathrm{z}_{22}^{\mathrm{b}} + \mathrm{z}_{22}^{\mathrm{c}} & \mathrm{z}_{21}^{\mathrm{c}} & 0 \\ 0 & 0 & -\mathrm{z}_{12}^{\mathrm{c}} & -\mathrm{z}_{11}^{\mathrm{c}} - \mathrm{z}_{11}^{\mathrm{d}} & -\mathrm{z}_{12}^{\mathrm{d}} \\ 0 & 0 & 0 & \mathrm{z}_{21}^{\mathrm{d}} & \mathrm{z}_{22}^{\mathrm{d}} + z_L \end{vmatrix}$$

$$\mathrm{D}_1 = \begin{vmatrix} 0 & \mathrm{z}_{12}^{\mathrm{a}} & 0 & 0 & 0 \\ \mathrm{N} & \mathrm{z}_{22}^{\mathrm{a}} - \mathrm{z}_{11}^{\mathrm{b}} & -\mathrm{z}_{12}^{\mathrm{b}} & 0 & 0 \\ 0 & \mathrm{z}_{21}^{\mathrm{b}} & \mathrm{z}_{22}^{\mathrm{b}} + \mathrm{z}_{22}^{\mathrm{c}} & \mathrm{z}_{21}^{\mathrm{c}} & 0 \\ -\mathrm{N} & 0 & -\mathrm{z}_{12}^{\mathrm{c}} & -\mathrm{z}_{11}^{\mathrm{c}} - \mathrm{z}_{11}^{\mathrm{d}} & -\mathrm{z}_{12}^{\mathrm{d}} \\ 0 & 0 & 0 & \mathrm{z}_{21}^{\mathrm{d}} & \mathrm{z}_{22}^{\mathrm{d}} + z_L \end{vmatrix} \tag{5}$$

$$D_2 = \begin{vmatrix} \mathrm{z}_{11}^{\mathrm{a}} - z_B & 0 & 0 & 0 & 0 \\ \mathrm{z}_{21}^{\mathrm{a}} & \mathrm{N} & -\mathrm{z}_{12}^{\mathrm{b}} & 0 & 0 \\ 0 & 0 & \mathrm{z}_{22}^{\mathrm{b}} + \mathrm{z}_{22}^{\mathrm{c}} & \mathrm{z}_{21}^{\mathrm{c}} & 0 \\ 0 & -\mathrm{N} & -\mathrm{z}_{12}^{\mathrm{c}} & -\mathrm{z}_{11}^{\mathrm{c}} - \mathrm{z}_{11}^{\mathrm{d}} & -\mathrm{z}_{12}^{\mathrm{d}} \\ 0 & 0 & 0 & \mathrm{z}_{21}^{\mathrm{d}} & \mathrm{z}_{22}^{\mathrm{d}} + z_L \end{vmatrix}$$

$$\vdots$$

$$\vdots$$

$$D_5 = \begin{vmatrix} \mathrm{z}_{11}^{\mathrm{a}} - z_B & \mathrm{z}_{12}^{\mathrm{a}} & 0 & 0 & 0 \\ \mathrm{z}_{21}^{\mathrm{a}} & \mathrm{z}_{22}^{\mathrm{a}} - \mathrm{z}_{11}^{\mathrm{b}} & -\mathrm{z}_{12}^{\mathrm{b}} & 0 & N \\ 0 & \mathrm{z}_{21}^{\mathrm{b}} & \mathrm{z}_{22}^{\mathrm{b}} + \mathrm{z}_{22}^{\mathrm{c}} & \mathrm{z}_{21}^{\mathrm{c}} & 0 \\ 0 & 0 & -\mathrm{z}_{12}^{\mathrm{c}} & -\mathrm{z}_{11}^{\mathrm{c}} - \mathrm{z}_{11}^{\mathrm{d}} & -\mathrm{N} \\ 0 & 0 & 0 & \mathrm{z}_{21}^{\mathrm{d}} & \mathrm{z}_{22}^{\mathrm{d}} + z_L \end{vmatrix}$$

The material parameters of the Langevin transducer used in the equivalent circuit and FEM analysis are shown in the Table 1.

Table 1. *Material parameters of the Langevin transducer.*

Material	Density(kg/m^3)	Young's modulus(N/m^2)	Acoustic velocity(m/s)	Natural acoustic impedance (Mrayl)	Poisson ratio
Iron	$\rho_a = 7800$	$E_a = 2.1 \times 10^{11}$	$c_a = 5188$	40.47	0.28
Aluminum	$\rho_d = 2700$	$E_d = 7.7 \times 10^{10}$	$c_d = 5340$	14.42	0.32
Water	$\rho_L = 1000$		$c_L = 1500$	1.5	
Air	$\rho_B = 1.29$		$c_B = 340$	4×10^{-4}	
		Flexibility	(m^2/N)	Piezoelectric modulus	(c/N)
		$\mathrm{s}_{11}^{\mathrm{E}}$	10.97×10^{-12}	d_{31}	-74.02×10^{-12}
Piezoelectric		$\mathrm{s}_{12}^{\mathrm{E}}$	-3.3×10^{-12}	d_{33}	181.11×10^{-12}
ceramic	$\rho = 7746$	$\mathrm{s}_{13}^{\mathrm{E}}$	-5.37×10^{-12}	d_{15}	505.16×10^{-12}
(PZT-M)		$\mathrm{s}_{33}^{\mathrm{E}}$	15.44×10^{-12}	Relative permittivity	
		$\mathrm{s}_{44}^{\mathrm{E}}$	39.59×10^{-12}	$\varepsilon_{11}^{\mathrm{T}}/\varepsilon_0$	1385
		$\mathrm{s}_{66}^{\mathrm{E}}$	28.53×10^{-12}	$\varepsilon_{33}^{\mathrm{T}}/\varepsilon_0$	713

In order to obtain the optimal dimension of front and rear plates for the maximum ratio $\vartheta_2^{\mathrm{d}}/\vartheta_1^{\mathrm{a}}$ of vibrating velocity in the front and back radiating sides from the equation (3) of Mason equivalent circuit we considered the change of vibrating velocity ratio according to the change of length in the front and rear plates under the condition that satisfies the frequency equation $|\mathrm{D}| = 0$ in operating frequency 20kHz. And the result is shown in the Figure 3.

Also we showed the change of the vibrating velocity ratio according to length change of the front and rear plates under the condition that satisfies the resonance frequency 20kHz using ANSYS. The transverse axis in Figure 3 is the length-axis of the transducer's rear plate, the left side of longitudinal axis is the vibrating velocity ratio-axis and the right side is the length-axis of the front plate. Curve ① in Figure 3

obtained from the equivalent circuit analysis is the change curve of the vibrating velocity ratio according to the length variation of the front and rear plates and curve ③ obtained from the FEM analysis is the change curve of the vibrating velocity ratio in the transducer's front and back radiating sides.

Curve ② in Figure 3 shows the relation between the dimensions of the front and rear plates when the above condition is satisfied.

As shown in Figure 3, vibrating velocity ratio of the Langevin transducer (boltless) radiating in the medium obtained from the Mason equivalent circuit analysis has a maximum value of about 1.94 when the lengths of the front and rear plates are L_d=30mm and L_a=72mm respectively. And, for the front and rear plate's lengths of BLT satisfied the resonance frequency 20kHz, the length of the rear plate is decreased from 100 to 0mm when the length of the front plate is increased from 0 to 100mm.

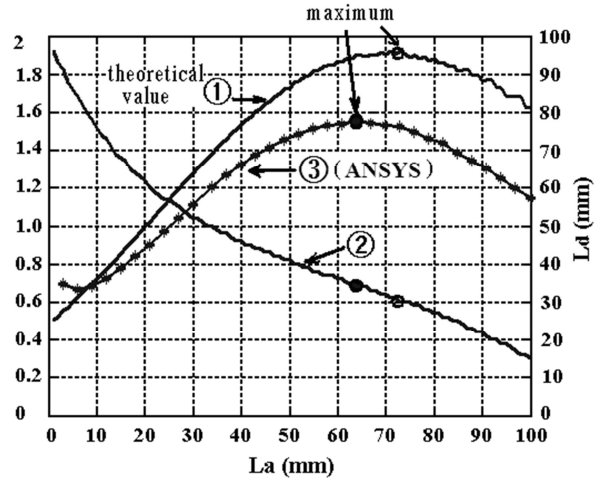

Figure 3. *The ratio of vibrating velocities according to the change in the length of front and rear plates of the transducer and a relation.*

2. ANSYS Analysis and Experimental Verification

We carried out ANSYS analysis on the vibrating velocity ratio according to the change in the length of front and back plates of BLT in radiating medium and compared it with the above theoretical results. Then proceeded the analysis of acoustic field of the transducers with the geometrical structure for the maximum vibrating velocity ratio.

Material characteristics of BLT and radiating medium utilized in ANSYS analysis are shown in the Table 1.

The front and back radiating mediums are water and air respectively. In the ANSYS analysis, we considered the BLT to is one-sided vibrating system because the characteristic impedance of water awfully lager than one of air.

The axisymmetric 2-D element types Plane226 and Plane82 are used for element types of piezoceramics and the front and rear plates. And Plane29 and Plane129 are used for element types of radiating medium and boundary lines of the infinite medium. Total number of elements of the transducer and medium is about 30 000 and the driving voltage of 1V was applied to the piezoceramics as boundary condition. Here the radius of the farthest medium boundary satisfies the condition of infinite medium acoustic field ($R \geq 2\emptyset_d{}^2 f_r/c_L$). (R=0.3m)

We regarded the coefficient of loss of transducer as 0.6%, the symmetric axis of 2-D axisymmetric model of transducer as Z-axis and the vibrating direction as Y-axis and carried out the harmonic analysis. And we made an analysis of the material parameters of the piezoceramics changing the direction of polarization from Z-axis to Y-axis.

First we carried out an analysis of acoustic field in radiating medium when the lengths (Ld, La) of the front and rear plates of BLT are changed according to the curve ② in Figure 3. And the changes of vibrating velocity ratio in the front and back sides of transducers was investigated.(curve ③ in the Figure 3)

As shown in the curve ③ in the Figure 3, the change of vibrating velocity ratio of the front and back sides of BLT which radiates one-sidedly showed a similar behavior to the equivalent circuit theory (curve①), but had a maximum value of 1.54 when the front and back lengths are $L_d = 64$mm and $L_a = 34$mm respectively.

The curve ① is obtained from the equivalent circuit of 1-D piston vibration of boltless Langevin transducer and the curve ③ is obtained from 2-D finite element analysis of the BLT with both longitudinal and bending vibration. This results in the difference of curves ① and ③.

Next, we showed the result of acoustic field analysis of the BLT with a structure for the maximum vibrating velocity ratio ($L_d = 64$mm, $L_a = 34$mm) and an operating frequency of 20kHz when one-sidedly radiating in the medium.

Figure 4 shows the model of axisymmetric 2-D acoustic field analysis of the BLT in radiating medium.

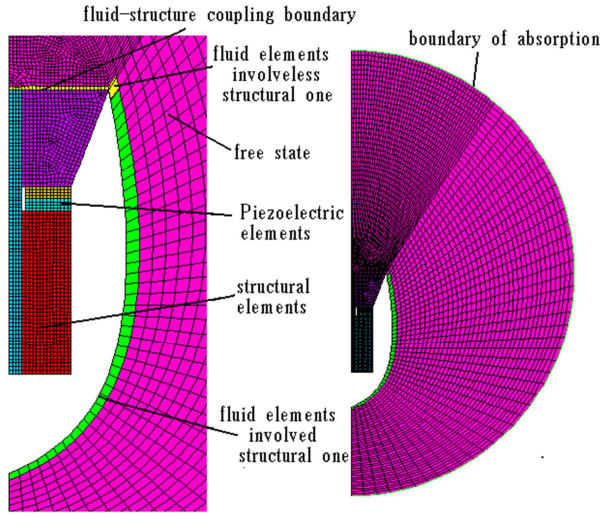

Figure 4. *Axisymmetric 2-D model of acoustic-field analysis of the BLT (Y-axisymmetric).*

As shown in Figure 4, we used the fluid elements involved structural elements for the boundary between BLT and

medium of fluid (fluid-structure coupling boundary), between medium of fluid and free space. And we used the fluid elements excluded from structural elements for the other medium of fluid.

And the number of partitions in the zone of transducer's front radiating medium was chosen much more than side face and back radiating medium of transducer in order to attain accurate distribution of acoustic pressure on the central axis of transducer's radiating side.

We obtained the electric charge on the upper and lower electrode of transducer using harmonic analysis and calculated the conductivity following the frequencies. And we calculated distribution of acoustic pressure and directivity obtaining the values of acoustic pressure according to polar coordinates from the acoustic axis of transducer (central axis of transducer's radiating side) to the angles of 180 degrees on infinite medium boundary.

Figure 5 shows the conductivity curve of BLT with the lengths of head and tail section L_d=34mm, L_a=64mm respectively when it radiates one-sidedly in the water.

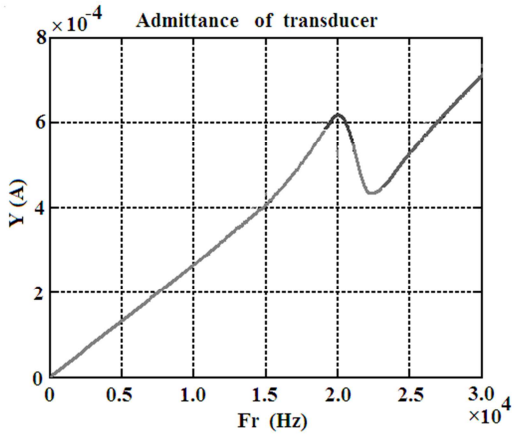

Figure 5. *Conductivity curve of transducer radiating one-sidedly in water.*

The conductivity curve of Figure 5 was obtained from harmonic analysis of one-sidedly radiating BLT in water with 100Hz interval in 0~30kHz range using the ANSYS and MATLAB software.

As shown in Figure 5, resonance and antiresonance frequencies of the transducer in underwater are fr=20kHz and fa=22.4kHz, effective electrical electromechanical coefficient of association keff is keff=0.45 from $k_{eff}^2 = 1 - \frac{f_r^2}{f_a^2}$, -3dB frequency band-pass is f2-f1=5.98kHz and its quality-factor is Qw=fr/(f2-f1)=3.17. Maximum conductivity in resonance is Gw=0.65mS, equivalent effective impedance, capacitance and inductance are Rw=1/Gw=1.54 kΩ, Cw=1/(2π×fr×Qw×Rw)=1.63nF and Lw=Qw×Rw/(2π×fr)=38.9mH respectively.

Figure 6 shows the distribution of acoustic field and directivity for one-sidedly radiating BLT obtained from acoustic field analysis. And the assembled BLT is shown in Figure 7.

The conversion efficiency of the BLT is above 90% and the radiating power is high as 130W. The ultrasonic processor made using the BLTs is also shown in Figure 8. Total 12 transducers were used for the device and the power consumption is 1500W.

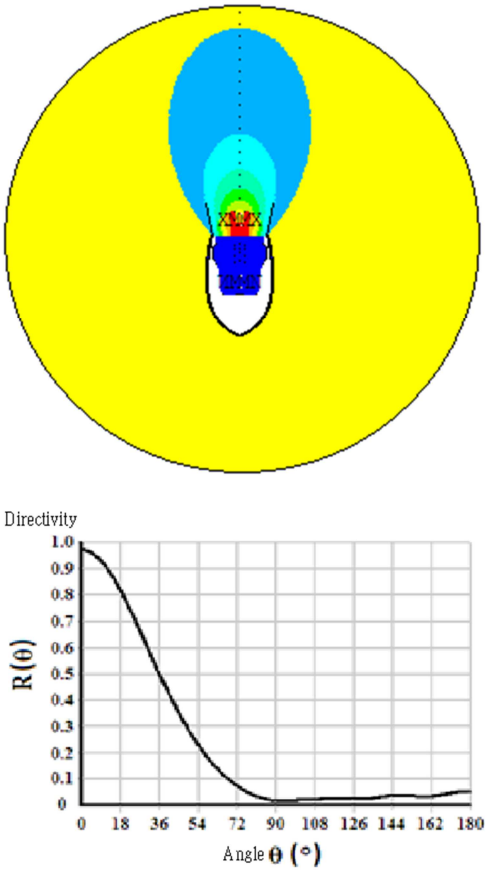

Figure 6. *Distribution of acoustic field and directivity for one-sidedly radiating BLT in the medium.*

Figure 7. *Assembled BLT.*

Figure 8. *Ultrasonic processor made using the BLTs.*

3. Conclusion

In this paper, we studied the geometrical structure of the front and rear plates of BLT for the maximum vibrating velocity ratio to obtain the maximum radiating power in operating frequency 20kHz using the Mason equivalent circuit analysis and finite element analysis.

We also established a theory for the design of the geometrical structure for the maximum carrier-power which is applicable to not only the half wavelength resonance system but also the further ones.

And we produced the BLT with the front and rear plates size of 34mm and 64mm respectively, operating frequency of 20 kHz and radiating power of 130W.

References

[1] Sergei L. Peshkovsky, Alexey S. Peshkovsky: Matching a transducer to water at cavitation: Acoustic horn design principles, Ultrasonics Sonochemistry 14 (2007) 314–322.

[2] Zhiqiang Fu a, Xiaojun Xian a,b, Shuyu Lin a,: Investigations of the barbell ultrasonic transducer operated in the full-wave vibrational mode, Ultrasonics 52 (2012) 578–586.

[3] R. P. Taleyarkhan, C. D. West, J. S. Cho, R. T. Lahey Jr., R. I. Nigmatulin, R. C. Block, Science 295 (2002) 1868.

[4] D. J. Flannigan, K. S. Suslick, Nature 434 (2005) 52.

[5] T. J. Mason, Ultrason. Sonochem. 10 (2003) 175.

[6] U. S. Bhirud, P. R. Gogate, A. M. Wilhelm, A. B. Pandit, Ultrason. Sonochem. 11 (2004) 143.

[7] S. Sherrit, S. A. Askins, M. Gradziol, B. P. Dolgin, X. B. Z. Chang, Y. Bar-Cohen, in: Proceedings of the SPIE Smart Structures Conference, San Diego, CA 4701, Paper No. 34, 2002.

[8] L. Parrini, New technology for the design of advanced ultrasonic transducers for high-power applications, Ultrasonics 41 (2003) 261-269.

[9] A. Lula, G. Caliano, A. Caronti, M. Pappalardo, A power transducer system for the ultrasonic lubrication of the continuous steel casting, IEEE Transactions on Evolutionary Computation 50 (2003) 1501-1508.

[10] J. Woo, Y. Roh, K. Kang, S. Lee, Design and construction of an acoustic horn for high power ultrasonic transducers, in: Proceedings of 2006 IEEE Ultrasonics Symposium, 2006, pp. 1922-1925.

[11] B. Fu, t. Hemsel, J. Wallaschek, Piezoelectric transducer design via multiobjective optimization, ultrasonics 44 (2006) e747-e752.